International Journal of Latest Engineering and Management Research (IJLEMR)
ISSN: 2455-4847
www.ijlemr.com ‖ Volume 1 - Issue 8 ‖ September 2016 ‖ PP. 07-28

Influence of Atmospheric Turbulence on Laser Range Evaluations

Hassan H.Mohammed[1] & Sadeq A.Rashid[2]
[1]*Department of Computer Technology Engineering, Iraq University College, Alestiqlal Street, Basrah, Iraq*
[2]*Department of Physics, College of Science, Basrah University, Basrah, Iraq*
Correspondence: Hassan H.Mohammed,Department of Computer Technology Engineering, Iraq University College, Alestiqlal Street,Basrh,IRAQ.

Abstract: In this paper, the modifications of the traditional range equations are investigated by taking into consideration the atmospheric turbulence, and the beam spot radius at the transmitter. The combination of these two factors is shown to be a potentially contributors to the laser range evaluations. The results of received power at the detector surface area are compared in both cases with and without turbulence. Using the corrective factors for the laser range equation (LRE), the received red power shifts due to turbulence relative to the free space received power are calculated. These red shifts are shown for the first time to be a metric ruler for the direct range evaluation. A statistical approach for evaluating the cosine angle between the normal to the target surface relative with laser receiving axis ($\cos\varphi$) is made.

Keywords: Laser range equation, Atmospheric turbulence effects, Received power shifts, Corrective factors.

1. Introduction

Laser rangefinder (LRF) is a device, which uses a laser pulse to determine the distance to an object. It is one of the first and successful applications of laser technology in the civilian and military applications [1]. In practice, there are many methods to measure distance using laser light, these methods are: interferometers, phase shift, triangulation, and time-of-flight measurements [2, 3]. All techniques are shared on the transmission of a short pulse of electromagnetic radiation towards certain diffused target and analysis of the back scattered signals from this target to determine the range. This technique is called the time of flight TOF , which is the most used laser ranging technique. The constant speed of light c , and an accurate measurement of the time taken between transmitter and target Δt , the range R can be measured on the bases of the relation $R = c\Delta t / 2$ [3-5]. Generally, the accuracy of laser range measurement is affected by a number of factors, including signal strength, noise in the electronics, and target reflectivity. By identifying and quantifying these factors, highly accurate range data of objects can be acquired [4, 5]. In addition to these internal effects, external effects are available such as rain, snow, sleet, fog, haze, pollution, etc., these atmospheric factors affect viewing of distant objects. The three primary atmospheric processes that affect optical wave propagation are *absorption*, *scattering,* and *refractive-index fluctuations* (atmospheric optical turbulence) [5]. Absorption and scattering by the constituent gases and particulates of the atmosphere give rise primarily to attenuation of the laser beam. Theories relating to atmospheric turbulence have been studied over many decades in order to better understand the impact of turbulence on the propagation of a laser beam through the atmosphere [5-7]. Index of refraction fluctuations lead to irradiance fluctuations, beam broadening, and loss of spatial coherence of the optical wave, among other effects. Clearly, these deleterious effects have far-reaching consequences on the use of lasers in optical communications, imaging, remote sensing, laser radar, and other applications that require the transmission of laser beams through the atmosphere. Nonetheless, the most serious optical effects on a propagating laser beam are generally those caused by small temperature variations that manifest themselves as index of refraction fluctuations [8].It should be mentioned that the laser range equations often produce unreliable predictions of the practical data, the primary reason for this inaccurate predictions is due to optical turbulence effects on the propagation beam [5].

In this paper the effect of atmospheric *turbulence, beam spot radius at transmitter is* introduced into the traditional radiometric three range cases namely, total reflection of the laser beam, partial reflection and Gaussian beam for extracting new formulations for these range cases. Also the maximum distance between the laser ranging system and the target, for different values of visibility range are evaluated. Although the laser range equation without the corrective factor provides a reasonable prediction for weak atmospheric turbulence conditions, it is shown in the present work that it decreases in accuracy as the refractive structure parameter increases into the moderate and strong regimes at a specific wavelength. The calculations are implemented by MATLAB software.

2. Laser Range Equations

2.1 Total reflection

For a point source transmitter , at the same place with receiver plane, the total reflected signal from a diffuse target is subjected to Lambert's law (beam spot radius is smaller than the target area) , the receiving power at detector is given by [1, 2 , 9 ,10,11]

$$P_D = \frac{D^2 \eta_t \eta_r \rho \cos\varphi P_t}{8R^2} \tau_a{}^2(\lambda, R) \quad (1)$$

This is the near range equation, where P_D represents the power of reflected signal at detector in(watt) , D is the receiver diameter in (m) , ρ target reflectivity, η_t and η_r optical efficiency of transmitter and receiver respectively , φ is the angle between the transmitted beam line and the normal to the diffuse reflecting target, P_t is the signal power at transmitter in (watt) , A_D is the detector area in(m^2) , $\tau_a{}^2$ atmospheric transmittance factor in two ways laser propagation (from transmitter to target and from target to receiver) as a function of laser wavelength λ and range R which refers to the distance between the target and receiver system called "range" R , and $2\pi R^2$ represents the laser beam area at the target .

2.2 Partial reflection

In general cases of the long range measurements, the transmitted laser beam diverges such that its diameter becomes larger than the target dimension. Consequently, the beam is only partially reflected by the target, therefore the target reflects only a portion of the transmitted power. Thus the physical range equation for *a partial reflected beam* (far range) can be rewritten as [1, 12, and 13]:

$$P_D = \frac{D^2 \eta_t \eta_r \rho \cos\varphi P_t A_{tar}}{8\pi\theta^2 R^4} \tau_a{}^2(\lambda, R) \quad (2)$$

This is the far range equation, where θ represents the half divergence angle in (rad.), A_{tar} is the area of the target in (m²). Eqs. (1 and 2) represent physical laser range equations providing optical power of the Lambertian target. These approximate equations are widely used in range evaluation [1, 2, 5, and11] but suffer from the neglect of many factors:

i- Both equations did not take into consideration several additional aspects of laser range finding, like atmospheric turbulence, beam spot radius at transmitter, and size of the target in relation to laser spot.

ii- The dimensions of a target must be known before shooting, for high range accuracy measurements using Eq. (2).

These two aspects are taken into account in the present work by introducing factors which calculate the influence of atmospheric turbulence along with the effect of beam spot radius at transmitter.

2.3 Gaussian Laser Range Equation

In the absence of optical turbulence (free space), the diffractive beam spot radius at distance z from transmitter is given by [7, 8]:

$$W(z) = W_\circ[(1-\frac{z}{F_\circ})^2 + (\frac{2z}{kW_\circ{}^2})^2]^{1/2} \quad (3)$$

$W_\circ$ represents beam spot radius at transmitter (z = 0) , defined as the point at which the field amplitude is $1/e$ of that observed on the optical axis , i.e. the beam center , and $F_\circ$ is the face front radius of curvature at the transmitter , and k is the propagation constant ($2\pi/\lambda$) in(m^{-1}). In case of divergent beam ($z/F_\circ \approx 1$), Eq. (3) can be re-written as [8]:

$$W(z) = W_\circ[1+(\frac{2z}{kW_\circ{}^2})^2]^{1/2} \quad (4)$$

For a Gaussian beam in far-field conditions (i.e., z large), $2z / kW_{\circ}^{2} >> 1$, Eq.(4) can be approximated to [2]:

$$W(z) = \frac{2z}{kW_{\circ}} = \frac{\lambda z}{\pi W_{\circ}} \quad (5)$$

In terms of half beam divergence angle θ , Eq. (5) written as [2]

$$W(z) = \theta z \quad (6)$$

Where:

$$\theta = \frac{2}{kW_{\circ}} = \frac{\lambda}{\pi W_{\circ}} \quad \text{(In radian)} \quad (7)$$

Eq. (5) and Eq. (7) clearly indicated that, a small beam radius $W_{\circ}$ will produce a large beam divergence [4]. *Sahapong* and *Widjaja* [1] estimated a new LRF equation corresponding to a Gaussian beam profile model using $1/e^2$ the point of irradiance to define the beam spot size as:

$$P_D = \frac{D^2 \eta_t \eta_r \rho \cos\varphi P_t}{8R^2} \cdot [1 - \exp(-\frac{2r^2_{tar}}{\theta^2 R^2})] \cdot \tau_a{}^2(\lambda, R) \quad (8)$$

This is the Gaussian range equation, where r_{tar} is the target's radius in (m). Eq. (8) used to calculate the range for near and far distances .This equation needs to introduce the corrective factors of the atmospheric turbulence and the beam spot radius at transmitter. These two factors are taken into accounts in both ground to ground (g-g) propagation and the slant path propagation (g-a). In addition, a new method for estimating the value of ($\cos\varphi$) is demonstrated, and the comparison with the other approaches are made.

3. *Atmospheric optical turbulence*

Turbulent atmosphere can be represented as a set of vortices , or eddies , of various scale sizes, extending from a large scale size $L_{\circ}$ called the *outer scale* of turbulence , to a small scale size l_o called the *inner scale* of turbulence [7,14] . Therefore the optical turbulence in the atmosphere can be characterized by three parameters: l_o, $L_{\circ}$, as well as the structure parameter of refractive index fluctuation c_n^2 . The inner scale is defined as the size of the smallest atmospheric eddies and its value near the ground is typically observed to be around (3 to 10 mm), but generally increases to several centimeters with increasing the height above the ground h . The outer scale is defined as the size of the largest atmospheric eddies for which atmospheric turbulence may still be considered isotropic and usually taken to be roughly $(h/2)$. Some models predict maximum values of outer scale between 4 and 5 meters and others predict the outer scale can be several hundred meters or more [10]. As a laser beam propagates through the path from the transmitter to the target and back to the receiver, the beam encounters random fluctuations in the refractive index of the atmosphere due primarily to temperature differences along the path. Therefore the effect of atmospheric turbulence on the target return power received by a laser rangefinder may be characterized by the parameters c_n^2 , l_o , λ and receiver diameter D. These parameters are of a major importance on the received power and consequently on the range accuracy at 1.54 μm [12, 14], and are numerically simulated in the present work.

3.1 Refractive index structure parameter

Refractive index structure c_n^2 is considered as a key for the information about the way in which beam is affected by turbulence. This parameter changes as a function of altitude and alters the behavior of the aberrations. As c_n^2 increases, so does the effect of the beam spot aberration typically, c_n^2 decreases in relation to altitude [7]. The refractive index alone provides adequate information about the turbulent region in horizontal path. Therefore c_n^2 used to distinguish between three turbulence regimes where $c_n^2 < 10^{-17} m^{-2/3}$

in the weak turbulence and $10^{-17} m^{-2/3} \le c_n^2 \le 10^{-13} m^{-2/3}$ in the moderate turbulence and $c_n^2 > 10^{-13} m^{-2/3}$ in the strong turbulence [6, 15].

Values of c_n^2 near the ground in warm climates generally vary between $10^{-14} m^{-2/3}$, and $10^{-12} m^{-2/3}$ the latter of which is considered strong turbulence in many regions [12]. Environmental effect of c_n^2 is characterized by three main parameters: the time of day, altitude above ground level, and wind speed [5]. The minimum value of c_n^2 is at sunrise and sunset when air temperature is closest to ground temperature. Temperature gradient is generally greatest at midday and midnight when ground is warmer than overlying air, thus increasing c_n^2 . As the altitude increases, the temperature gradient decreases, resulting of a minimum c_n^2 [6]. Mathematically, several $c_n^2(h)$ profile models have been developed over the years, one of these is the well known Hufnagel-Valley (H-V) model [7, 14, 15]

$$c_n^2(h) = 8.148\times10^{-56} v^2 h^{10} \exp(-\frac{h}{1000}) + 2.7\times10^{-14} \exp(-\frac{h}{1500}) + c_n^2(0)\exp(-\frac{h}{100}) \quad (9)$$

h is the altitude above the ground level in (m) , v is the surface wind speed (in m/s) , and $c_n^2(0)$ is the normal value of $c_n^2(h)$ at the ground level where $c_n^2(0) = 1.7\times10^{-14} m^{-2/3}$ is considered as typical value of c_n^2 when $h = 0$ and $v = 21 m/\sec$ [14,16] . In case of laser range, the typical propagation path of laser beam is often a horizontal, near ground path, therefore the atmospheric turbulence for this type of path frequently falls into what is categorized as strong fluctuation conditions due to large temperature differences between the earth ground level and the surrounding air [5].

3.2 Scintillation

Scintillation can be classified as random intensity fluctuations caused by fluctuations experienced in the received irradiance when light beams propagate through a turbulent atmosphere. Measuring certain observations in the laboratory allows the scintillation to be calculated by Rytov variance σ_R^2 , assuming $l_\circ = 0$, $L_\circ = \infty$ and constant c_n^2 along the propagation path, σ_R^2 can be written [4, 7, 12,17]

$$\sigma_R^2 = \frac{< I^2 >}{< I >^2} - 1 = 1.23 c_n^2 k^{7/6} z^{11/6} \quad \text{(unitless)} \quad (10)$$

σ_R^2 is the Rytov variance gives a variance for the log intensity fluctuations at $l_\circ = 0$, I is the signal irradiance (or intensity) seeing by point detector. The notation here indicates that this is a variance of intensity fluctuations, and z is the total propagation path length of optical beam in (m) (= $2R$ in case of LRF), k is the wavenumber. The R subscript emphasizes that this variance holds in the Rytov regime, where the turbulence is weak. When the turbulence is not weak, it is still possible to refer to the Rytov variance, as calculated from Eq. (10) [7, 17]. We noted from Eq. (10), that the Rytov variance increases with an increase in c_n^2 at a constant R . Therefore, Rytov variance is customary used to distinguish between weak or strong fluctuation. In terms of this parameter the strength of turbulence is classified as $\sigma_R^2 >> 1$ in case of strong turbulence, $\sigma_R^2 = 1$ in case of moderate turbulence, and $\sigma_R^2 << 1$ in case of weak turbulence [12]

3.2.1 ***Effect of inner scale*** $l_\circ$ ***on scintillation***

For scintillation, only inner scale effects need to be considered, since large scale have little influence on scintillation effects. The true Rytov variance can be estimated as a function of the σ_R^2 and *the dimensionless Fresnel zone size,* δ $(\delta = \sqrt{\lambda z}/l_\circ)$ which represents the eddies size relative to the inner scale $l_\circ$, *an inner scale corrected Rytov variance* was found to be approximately [18]:

$$\sigma_R{}^2(\delta) = \sigma_R{}^2[1-\exp(-\frac{\delta^2}{\omega(\delta)})][0.48\exp(-\frac{\delta^2}{14.43})+1] \quad (11)$$

Where $\omega(\delta)$ is given by:

$$\omega(\delta) = 11.1 - 4.7\exp[-(\delta-1.7)^2/7.632] \quad (12)$$

Eq. (11) and Eq. (12) were developed using a graphical analysis technique to obtain an approximate expression. Using $\sigma_\chi{}^2$ and δ one can then compute the *irradiance variance* with $l_\circ$ as:

$$\sigma^2{}_I(\Psi) = [1-\exp(-\frac{\sigma_\chi{}^2}{\Psi})][(\Psi-1)\exp(-\frac{\sigma_\chi{}^2}{62.23})+1] \quad (13)$$

Where $\Psi(\delta) = 2.31 + 0.60\exp(5/\delta)$ (14)

3.2.2 Effect *of aperture-averaging on scintillation*

We have considered scintillation effects in the case of a very small (point) receiver aperture. However, the usual use of a large collecting aperture in laser range finder systems leads to reduced scintillation at the detector. This effect is called *aperture-averaging* [7, 19]. Aperture-averaging theory has been extensively developed for a plane wave in weak and strong turbulence conditions by Andrews et al [7]. They provided an empirical relation for aperture averaging factor in a double-pass scenario, by implementing the *ABCD* ray matrix approach in *weak turbulence medium*.

$$[A_{ap}]_{weak} = [1+1.062(k\frac{r^2{}_{rec}}{z})]^{-7/6} \quad (15)$$

Where r_{rec} is the radius of the receiver aperture in (m). So, when receiver-averaging is assumed, the variance of irradiance in case of weak turbulence can be calculated by multiplying the modified Rytov variance (Eq. 13) and the aperture-averaged factor (Eq. 15) as:

$$[\sigma_I{}^2]_{weak} = [A_{ap}]_{weak}\sigma_I{}^2(\Psi) \quad \text{(Under weak turbulence)} \quad (16)$$

On the other hand, Churnside [20] approximated the strong turbulence aperture-averaging factor as:

$$[A_{ap}]_{strong} = \frac{\sigma_I{}^2+1}{2\sigma_I{}^2}[1+0.9(\frac{r_{rec}}{\rho_\circ})^2]^{-1} + \frac{\sigma_I{}^2-1}{2\sigma_I{}^2}[1+0.61(\frac{k\rho_\circ r_{rec}}{z})^{7/3}]^{-1} \quad (17)$$

Where $\rho_\circ = [1.46k^2c_n{}^2z]^{-3/5}$ is the plane wave spatial coherence radius (Friend's parameter) in horizontal path for both weak and strong fluctuation regime in (m). Therefore, in the case of strong turbulence, the variance of irradiance can be written as:

$$[\sigma_I{}^2]_{strong} = [A_{ap}]_{strong}[\sigma_I{}^2(\Psi)] \quad \text{(Under weak turbulence)} \quad (18)$$

4. Effective Beam Spot Radius

Beam spreading due to pure diffraction W is described by Eq. (4). Additional beam spreading is due to optical turbulence is predicted by the mean irradiance assuming the neglect of the outer-scale effects. The effective beam size in both weak and strong turbulent regimes in horizontal path is given by [14]:

$$W_{eff} = W(1+T) = W[(1+1.33\sigma_R{}^2\Lambda^{5/6})]^{1/2} \quad \text{In (m)} \quad (19)$$

The additional term T describes the change in the on-axis mean irradiance at the receiver plane. In turbulence medium, $\Lambda = 2z/kW^2(z)$ is the Fresnel ratio. The effective beam spot radius W_{eff} is a measure of the effective turbulence induced beam spot size [16].

On the other hand, the laser beam propagation on slant path becomes very important when the parameter $c_n{}^2$ varies along the propagation path and the atmosphere being distributed non-uniformly, then Eq. (19) must be

developed [21]. When the laser beam propagates in slant path from ($z=0$ to $z=L$) , and by integrating the magnitude of $c_n^{\,2}(z)$ over a weighted path integral , then the additional parameter T is given by [7].

$$T = 4.35k^{\frac{7}{6}}(L\Lambda)^{\frac{5}{6}}\int_0^L c_n^{\,2}(z)(1-\frac{z}{L})^{\frac{5}{3}}dz \tag{20}$$

The resulting effective beam radius in slant path is given by:

$$W_{eff} = W\sqrt{1+4.35k^{7/6}(L\Lambda)^{5/6}\int_0^L c_n^{\,2}(z)(1-\frac{z}{L})^{5/3}dz} \tag{21}$$

Equation (21) is used to calculate the beam spot radius for laser beam propagates through turbulent slant path and refers to dependence of effective beam spot radius on propagation distance and altitude.

5. Atmospheric Turbulence Corrective Factor

The laser range equations described in Eqs. (1), (2) and (8) do not take into accounts for the effects of distorted beam properties. A corrective term that accounts for the difference in the intensity in the presence of atmospheric turbulence versus the irradiance due to free-space propagation was developed [8]. This term is defined as the ratio between power incident on the receiving aperture with atmospheric turbulence due to refractive-index fluctuations and the power incident on the receiving aperture after reflection from the target in free space due to diffraction effects alone, is given by [8]:

$$\tau_{turb} = \frac{P_{turb}}{P_{fs}} = \frac{1-\exp(-\frac{2r_{rec}^{\,2}}{W_{eff}^{\,2}})}{1-\exp(-\frac{2r_{rec}^{\,2}}{W_{rec}^{\,2}})} \quad \text{(unitless)} \tag{22}$$

W_{rec} is the beam radius of the reflected beam at the receiver plane in (m) ,which is calculated using the first minima of the beam's Airy diffraction pattern [5 , 22]

$$W_{rec} = \frac{1.22R\lambda}{D_{tar}} \tag{23}$$

Where D_{tar} , is the diameter of the target in (m). The corrective factor τ_{turb} is incorporated into the physical range equations for further correction to the characteristic effects of the turbulence on the beam.

6. Beam Spot Radius at Transmitter

In term of the beam parameters, the beam spot radius at distance z from the transmitter can be re-written as [8, 16, and 23]:

$$W(z) = W_\circ(\Theta_\circ^{\,2} + \Lambda_\circ^{\,2})^{1/2} \tag{24}$$

The transmitter parameters $\Theta_\circ = 1-(z/F_\circ)$, $\Lambda_\circ = 1-(2z/kW_\circ^{\,2})$ represents beam curvature parameter and Fresnel ratio entire in free space respectively. The radius of the beam waist W_b with a distance z_b from the plane of origin is given by [23]

$$W_b = W_\circ\frac{|\Omega_f|}{(1+\Omega_f^{\,2})^{1/2}} = \frac{W_\circ}{\sqrt{1+(\frac{kW_\circ^{\,2}}{2F_\circ})^2}} \tag{25}$$

And $\theta = \dfrac{\lambda}{\pi W_b}$ (at point b) (26) where $\Omega_f = 2F_\circ / kW_\circ^2$ is the beam focusing parameter . In a real situation, at relatively large propagation distance, $(kW_\circ^2 / 2F_\circ) >> 1$, and the divergence calculation using Eq.(33) reduces to ($\theta = W_\circ / F_\circ$) . Similarly, Eq. (6) could be expressed in a simplified form [19, 24, 25].

$$W(z) = W_\circ + \theta z \quad (27)$$

7. A modified Form of Laser Range Equations

As we mentioned before , φ represents the angle of target surface normal relative with laser receiving axis .Many researchers consider that the diffuse target plane and the laser rangefinder system is vertical, that is $\varphi = 0^\circ$ ($\cos\varphi = 1$) [2 , 26] . Or they suppose that the overall resultant value of $\cos\varphi$ may be approximated by 0.5 , depending on that the target does not have a flat surface but a topographical structure [1]. But in fact, it is very difficult to ensure that the diffuse target and the laser rangefinder system are vertical or the target has a topographical surface, that means $\varphi = 0^\circ$ or $\cos\varphi$ = 0.5. So the condition that the incident angle not equal zero also can bring the error to the value of sensitivity. As we can see from Fig. (1) , the $\cos\varphi$ part in equations depends on the surface roughness. When the measured area is flat then the incidence angle is the same as scan angle. The surfaces are assumed to have Lambertian backscattering properties. This means that the energy that is backscattered from the surfaces decreases with the increase of incidence angle. It is clear that those factors have to be taken into account when using the intensity data [27]

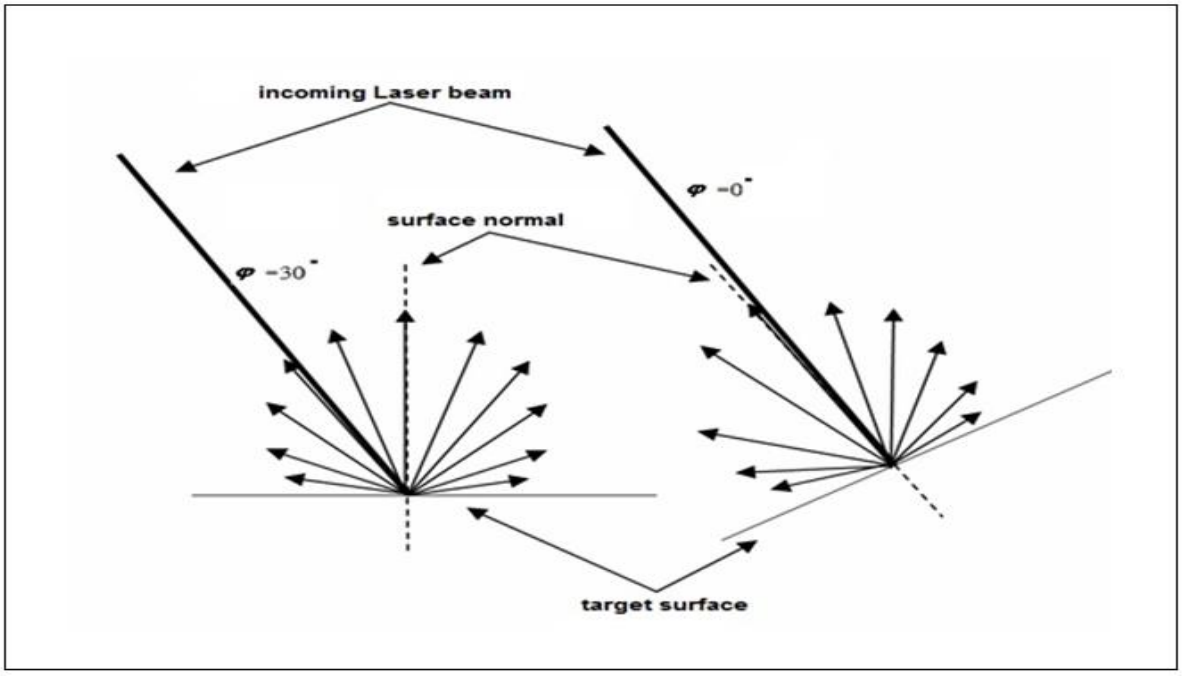

Fig.1: The variation in the angle φ =90º to -90º with incident laser beam to the normal on target surface [27].

In practice, the angle φ can be considered as a continuous random variable with the probability distribution function (P.D.F) as $f(\varphi) = \cos\varphi$. There are a number of useful functions with each probability distribution, and one of them is the *Cumulative Distribution Function* (CDF) .This function enables to calculate the probability of various outcomes, or events. By definition, the CDF indicates the probability the random variable X takes on a value less than or equal to x .The definition of the CDF is very simple that the CDF takes on values in the interval between (0, 1) .To calculate the probability that the variable X takes on a value more than x , we can use the following formula [28]

$$p(X > x) = 1 - p(X \le x) = 1 - p(x) \quad (28)$$

Similarly, we can calculate the probability that the random variable falls into some interval (x_1, x_2):

$$p(x_1 < X < x_2) = p(X \le x_2) - p(X \le x_1) \quad (29)$$

For continuous distributions, $p(X = x)$ always equals zero, so the expressions $p(X \le x)$ and $p(X < x)$ are equivalent and we can use the following formula:

$$p(x1 < X < x2) = p(x1 \le X \le x2) = p(x2) - p(x1) \quad (30)$$

Thus, in term of angle φ we have:

$$p(\varphi_\circ < \varphi < \varphi_1) == p(\varphi_1) - p(\varphi_\circ) \quad (31)$$

$p(\varphi)$ represents the probability of finding angle φ between values $\varphi_\circ$ .and φ_1 . Now we can re-write Eq. (31) in term of integral as:

$$p(\varphi_\circ < \varphi < \varphi_1) = \int_0^{\varphi_1} \cos\varphi d\varphi - \int_0^{\varphi_\circ} \cos\varphi d\varphi = \sin\varphi]_0^{\varphi_1} + \sin\varphi]_0^{\varphi_\circ}$$

$$= \sin\varphi_1 + \sin\varphi_\circ \quad (32)$$

We calculated the probability of variations in φ between many values of $\varphi_\circ$ and φ_1 ranging from (0°) to (90°) by the Eq. (32). The Cumulative probability as a function of φ was drowning in Fig. (2). the mean value of cumulative probability ≈ 0.1 for the ($0^\circ - 90^\circ$) range of φ. The same probability for the negative values of φ. The corresponding angle of the mean value of CDF is $\approx 49.9^\circ$ i.e. ($\cos\varphi$=0.64). This value is more accurate than the approximate value usually used by many references in laser range calculations without taking into account the statistical variations of the random variable of angle φ.

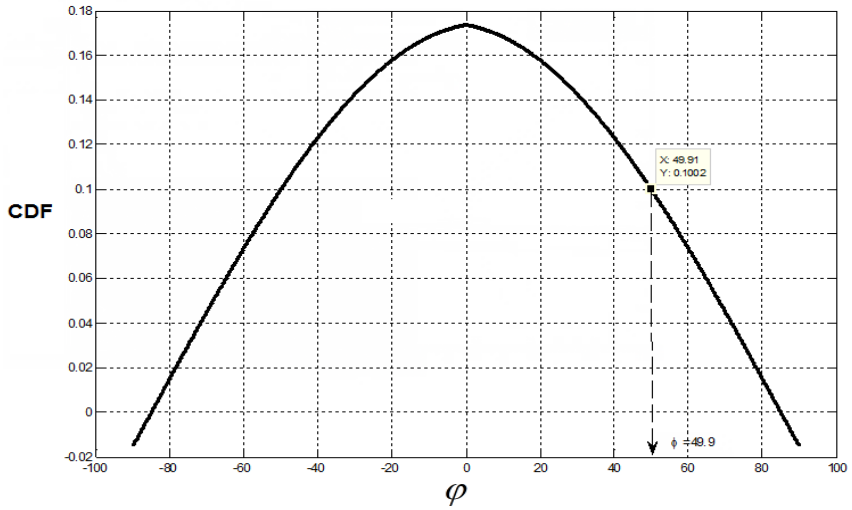

Fig. 2 .The cumulative probability as a function of φ

Another factor that must be taken into consideration is the shape factor P_{shape}. The confusion in this factor is introduced by the beam divergence based on the $1/e$ point of irradiance. The correct point of irradiance is based $1/e^2$ on the point of irradiance to define the beam spot size .In order to account for this; the factor P_{shape} that accounts for differences between the transmitted-beam-shape's resulting irradiance profile and an equivalent beam with uniform irradiance. For a Gaussian beam $P_{shape} = 2$ with beam divergence angle measured to the $1/e^2$ point of irradiance [5]. Taking into accounts the corrective factors for the effect of atmospheric turbulence, beam spot radius at transmitter, beam propagation factor, and the cosφ, one can re-write the LR equations (1),(2),and (8) in a new form as :

$$P_D = \frac{D^2 \eta_t \eta_r \rho \cos\varphi P_t P_{shape}}{8R^2} \tau_{turb.} \tau_a{}^2(\lambda, R) \quad \text{Total reflection} \quad (33)$$

$$P_D = \frac{D^2 \eta_t \eta_r \rho \cos\varphi A_{tar} P_t P_{shape}}{8\pi (W_\circ + \theta R)^2 R^2} \tau_{turb.} \tau_a{}^2(\lambda, R) \quad \text{Partial reflection} \quad (34)$$

$$P_D = \frac{D^2 \eta_t \eta_r \rho \cos\varphi P_t P_{shape}}{8R^2} [1 - \exp(-\frac{2r^2{}_{tar}}{(W_\circ + \theta R)^2}] \tau_{turb.} \tau_a{}^2(\lambda, R) \quad \text{Gaussian beam} \quad (35)$$

8. A New Form of a Gaussian Beam Equation

Theories relating to atmospheric turbulence effect have been studied over many decades in many researches in order to better understand the impact of turbulence on the propagation of a laser beam through the atmosphere [4, 6, 7, 16, and 17]. But all these available research were focused on the effect of turbulence on laser beam propagation through atmosphere or on Free Space Communication (FSO) performance , without referring to the impact of turbulence on *laser range* performance except few researchers .Cole and Haeri [5] were studied the turbulence effect using established theory, and developed a corrective term for use in the laser range equations that accounts for turbulence induced beam spreading and compared to experimental results . In the other hand, some researchers like Kruapech and widjaja [2] were developed a new Gaussian beam equation in free space without referring to the impact of turbulence in his calculations. Also, Li [29] proposed a novel method which can estimate the maximum range of laser ranging system without taken into account turbulence effect. However , in this work we have modified a new Gaussian laser range equation uses the turbulent medium for beam propagation ,and assuming that the laser signal propagates through a path as cone shape , it's head at laser source and base at target with radius (θR) where θ represents a half angle of beam divergence in (rad.) . Therefore, the area illuminated by cone spot light at distance R equals [π (θR) ²]. Consequently, the signal power at the circular target surface is given by [1, 2]

$$P_{tar} = A_{tar} \frac{P_t}{\pi(\theta R)^2} \quad (36)$$

in the presence of atmospheric turbulence effects, the irradiance of the radiation incident on the target surface, where the collecting lens in this case as a "*soft aperture*" lens or *Gaussian lens* is described by [14,16]

$$< I(r,z) >= I_\circ \frac{W_\circ^2}{W_{eff}{}^2} \exp(-\frac{2r^2}{W_{eff}{}^2})$$

(37)

Where r is the lateral distance from the center of the beam which is defined as ($\sqrt{x^2 + y^2}$) , $W_\circ$ is the beam spot radius at the transmitter , W_{eff} is given by Eq. (19) in case of ground horizontal , or by Eq.(21) in case of slant path , $I_\circ \equiv I(0,0)$ is The transmitted intensity at the centerline of the beam (with turbulence) defined as $I_\circ = 2P_{beam} / \pi W_{eff}{}^2$ [1,2,19] . In the presence of atmospheric turbulence between transmitter and target, the received signal power at the target plan can be approximated by [14]

$$P_{tar} = \int_0^{2\pi} \int_0^{\infty} < I(r,z) > r dr d\theta \quad (38)$$

Using the special integral $\int_0^{\infty} x^n e^{-ax^2} dx = \frac{\Gamma(\frac{n+1}{2})}{2a^{\frac{n+1}{2}}}$ along with Eq. (37), and $P_{beam} = P_t$ one can obtain:

$$P_{tar} = \frac{W_\circ^2}{W_{eff}{}^2} P_t = \frac{D^2}{4W_{eff}{}^2} P_t \quad \text{(Considering } W_\circ = D/2 \text{)} \quad (39)$$

Comparing Eq. (39) and Eq. (36) yields:

$$\frac{A_{tar}}{\pi(\theta R)^2} = \frac{D^2}{4W_{eff}{}^2} \tag{40}$$

Substituting Eq. (40) into Eq. (2), we obtain a new form of the range equation for a Gaussian beam in turbulent medium as:

$$P_D = \frac{D^4 \eta_t \eta_r \rho \cos\varphi P_t P_{shape}}{32 R^2 W_{eff}{}^2} \tau_a{}^2 \tag{41}$$

Eq.(41) is a new Gaussian reformulation of range equation in terms of receiver diameter D and the beam spot radius in turbulent atmosphere W_{eff} , that has never been reported before, taking into accounts turbulence parameters affecting the laser range finder system. The signal power at detector is inversely proportional to the square of the beam spot radius propagation through a turbulent atmosphere.

9. Simulation Results and Analysis

Numerical simulation of the influence of the governing parameters of the atmospheric turbulence, refractive index structure parameter, inner scale, and receiver aperture size on the received power of the LRF are studied. The laser wavelength λ= 1.54 μm is used. The comparison with the free space condition is made. Computer simulations are realized by the Matlab environment for the study of the turbulence effect and the free space atmosphere. The data given in Table (1) are used for the simulation program, and also show the values of the attenuation coefficient of atmosphere for various meteorological conditions at wavelength λ =1.54 μm [1, 14, 30, and 31].

The atmospheric scattering for the ground-to-ground transmission is calculated using the Beer's law [13, 32] which states that [$\tau_a(g-g) = \exp(-\sigma_a R)$], where τ_a is the atmospheric transmittance, σ_a is the scattering attenuation coefficient in (km^{-1}) and given by [13, 29]:

$$\sigma_a(\lambda) = \beta(\lambda) = -\frac{3.912}{R_v}\left(\frac{\lambda_{\mu m}}{0.55}\right)^{-q} \tag{42}$$

Thus, the exponential equation of atmospheric scattering transmittance as a function of visible range and laser wavelength is given by:

$$\tau_a(g-g) = \exp\left[-\frac{3.912}{R_v}\left(\frac{\lambda_{\mu m}}{0.55}\right)^{-q} R\right] \tag{43}$$

Where R_v is the horizontal visibility in (km), q is a parameter depends on volume contribution for particles in atmosphere and it is value equals (1.6) for $R_v > 50km$, (1.3) for $6km > R_v > 50km$ and equals ($0.585\sqrt[3]{R_v}$) for $R_v < 6km$. In addition to ground–to–ground transmission mode, there are two another laser transmission modes ground to air ($g-a$) and air-to-air ($a-a$) transmissions. When laser transmits from ground to air through free space, the atmospheric transmittance as a function of zenith angle and target's height h in (km) can be expressed as [13].

$$\tau_a(g-a) = \exp\{-\sec\theta_z\left(\frac{3.123}{R_v}\right)[1-\exp(-0.835h)]\} \tag{44}$$

Where θ_z is the zenith angle (the angle between the geographical vertical and incident directions in radian). Also, if the height of target and laser transmitter are h_1 , h_2 respectively, the air-to-air (a-a) atmospheric transmittance can be expressed as [13]:

$$\tau_a(a-a) = \exp\{\sec\theta_z\left(\frac{3.123}{R_v}\right)[\exp(-0.835h_2) - \exp(-0.835h_1]\} \tag{45}$$

Tables 1: System and target parameters used in the calculations and the International visibility code with corresponding attenuation coefficient values.

parameter	symbol	value	unit	Ref.
Laser wavelength	λ	1.54	μm	10
Laser pulse width	τ	6.5	$n\sec$	10
Laser peak power	p_t	0.33	MW	1,2
Half divergence angle	θ	0.6	$mrad.$	2
Receiver optical efficiency	η_r	0.45	--	1,2,28
Transmitter optical efficiency	η_t	0.85	--	1,2,28
Receiver aperture area	A_{rec}	1.6×10^{-3}	m^2	1,2
Receiver aperture radius	r_{rec}	0.025	m	1,2
Beam spot radius at the transmitter	$W_\circ$	0.025	m	6
Receiver aperture diameter	D	0.05	m	1,2,28
Target radius	$r_{tar.}$	1.15	m	1,2
Target area (NATO standard)	$A_{tar.}$	2.3×2.3	m^2	1,2
Target reflectivity	ρ	0.21	--	1,2
Typical refractive index structure parameter at ground level	$c_n^2(0)$	1.7X10^{-14}	$m^{-2/3}$	15
Refractive index structure parameter at ground level in strong turbulence	c_n^2	1X10^{-12}	$m^{-2/3}$	15
Refractive index structure parameter at ground level in weak turbulence	c_n^2	1X10^{-17}	$m^{-2/3}$	15

The International visibility code with corresponding attenuation coefficient values.

Weather condition	$R_v\,(km)$	$\sigma_a(\lambda)$ (km)	Ref.
Clear weather	23	0.1	1,2
Rain	2.8	1.059	19
Haze	1	3.17	19
Fog	0.5	6.65	19

9.1 Atmospheric transmission

It has been shown in the previous sections that the power received at the rangefinder detector mainly follows the atmospheric transmission. Accordingly, it becomes now important to know the behavior of this parameter at different atmospheric conditions to calculate the range performance. Using the Eq. (43), the change in ($g-g$) atmospheric scattering transmittance curve of 1.54 μm wavelength as a function of range is shown in Fig. (3). It can be noted the effect of the horizontal visibility variations on the laser propagation in the atmosphere. The transmission decreases exponentially with range increasing in low values of horizontal visibility R_v . In the case of clear weather conditions (R_v =23 km), the atmospheric transmission approaches high values and the curve approaches to straight line, while at poor visibility $R_v = 0.5km$, the atmospheric transmission decreases rapidly to minimum values as the range increases and approaching zero at high values of range. These behaviors are due to the linear scattering by aerosol constituents of the atmosphere (effect of aerosols attenuation).

Fig. (4) shows the ($g-a$) transmission as a function of range at clear weather conditions and different zenith angle using the Eq. (44). Obviously, in all cases when the transmission distance is increased, the atmospheric transmittance will be considerably decreased. At high zenith angle ($\square_z$=80º), the atmospheric

transmittance is much smaller than that at lower zenith angle levels because, at higher zenith angle, the transmission path is close to perpendicular to the ground and the relative height between laser source and target increases. This behavior is in agreement with that obtained in [13].

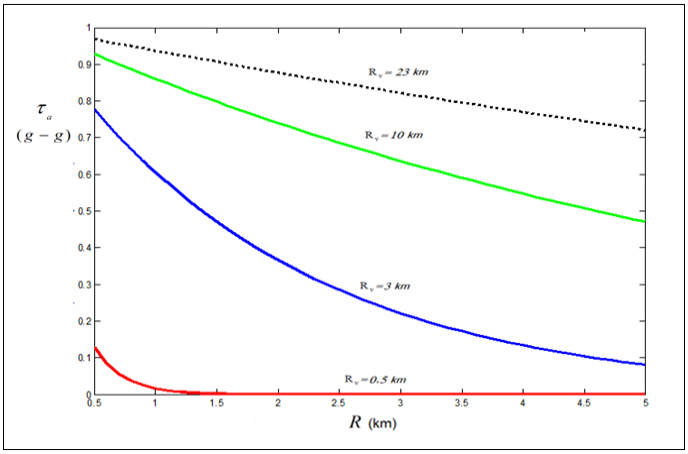

Fig. 3: Horizontal atmospheric scattering transmittance vs. range

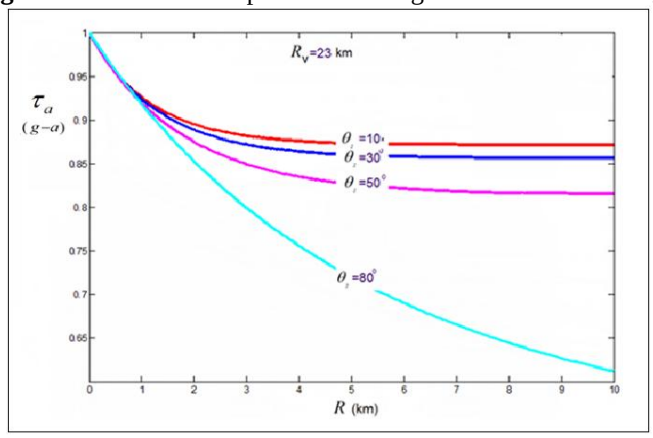

Fig. 4: Atmospheric transmission vs. range of ($g-a$) propagation at different values of zenith angles.

9.3 Effect of inner scale and aperture-averaging on scintillation.

Scintillation can be calculated by Rytov variance with zero-inner scale (Eq.10). Fig. (5) demonstrates the relation between the Rytov variance with the laser transmission distance in the case strong and weak turbulence. It can be noted that the scintillation rises against propagation distance, and gives high values more than 1000 in strong turbulence. Furthermore the effect of the turbulence on the scintillation index is more pronounced at large propagation distance and the turbulence decreases as refractive index parameter decreases.

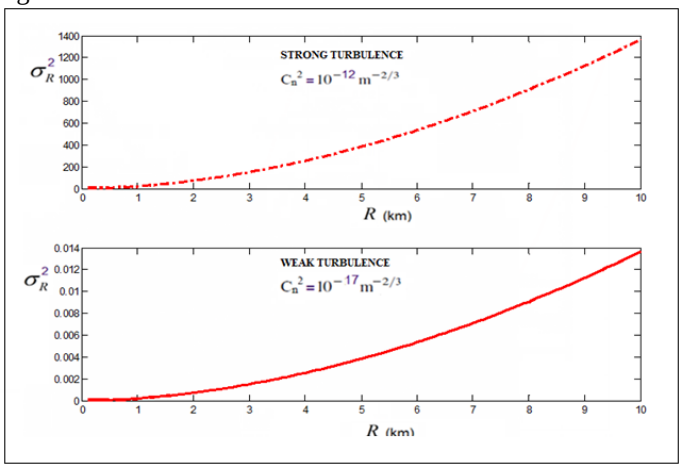

Fig 5: The relationship between Rytov variance σ_R^2 and the range (strong and weak turbulence)

Using Eq. (13), the relationship between the irradiance variance $\sigma^2_I(\Psi)$ with range in the case of strong and weak turbulence with non-zero inner scale, i.e., $(l_\circ = 3mm, l_\circ = 10mm)$ is illustrated in Figs. (6) and (7) respectively. Clearly, observe the distribution based on Eq. (13),but now much smaller irradiance values are obtained comparing with that computed by Eq. (10) in case of strong turbulence. The propagation path is assumed to be arbitrarily long and thus there is no remaining coherence in the wave, and this reduction in the beam coherence occurs due to the field perturbation at sufficient distance from the transmitter. Such an effect does not appear in the weak turbulence [33]. Simulation results of the Rytov variance given by Eq. (10) and that of Eq. (13) predicts a small error (≈ 0) when small path varying inner scale was introduced in case of weak turbulence, but this error increases with inner-scale increasing ,this clearly shown in the case of strong turbulence(Fig.6). The height of this peak depends on the value of δ used in Eq. (11). Eq. (3) has the proper asymptotic behavior, the peak of $\sigma^2_I(\psi)$ is situated at R=1km, gradually decreases to R=4km and remains constant at R□4km.

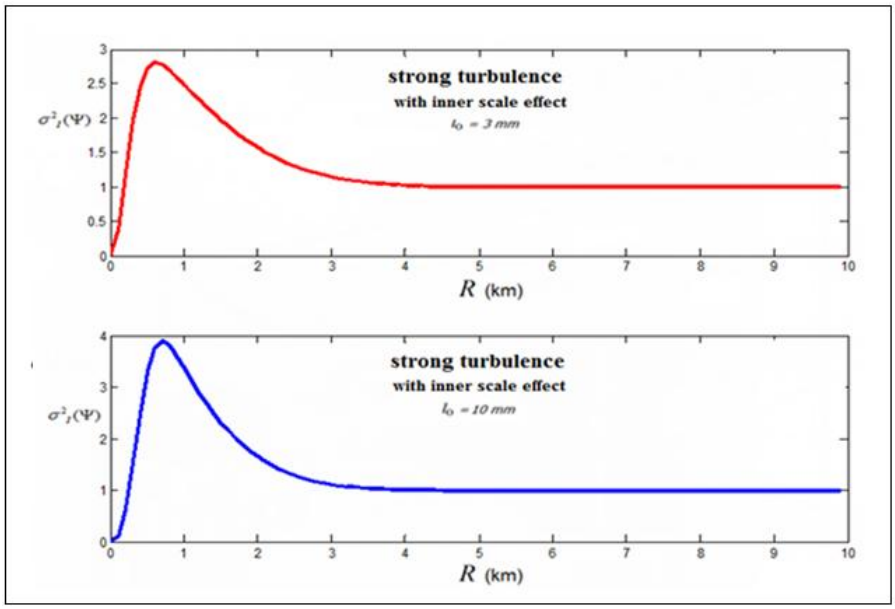

Fig 6: The relationship between the irradiance variance $\sigma^2_I(\Psi)$ and the range (strong turbulence).

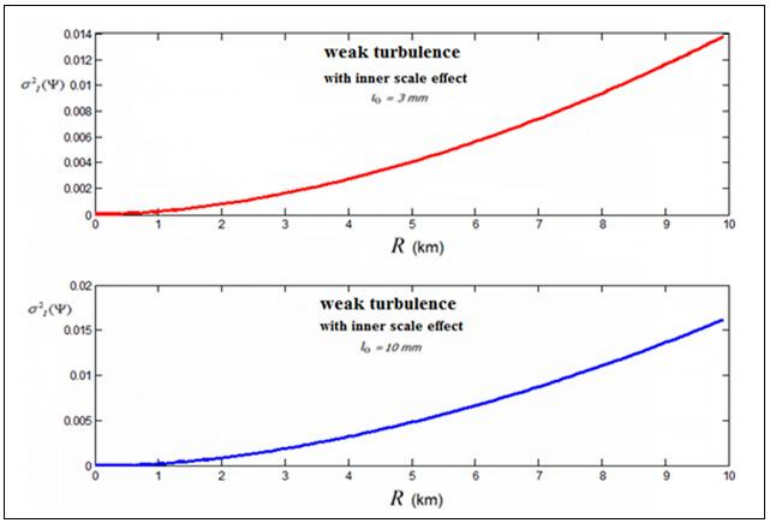

Fig 7: The relationship between the irradiance variance and the range (weak turbulence).

To investigate the effect of aperture-averaging on irradiance scintillations, the irradiance variance as a function of range with effect of aperture-averaging through strong turbulence $c_n^2 = 1\times10^{-12}\,m^{-2/3}$ (Eq.18) and weak turbulence $c_n^2 = 1\times10^{-17}\,m^{-2/3}$ (Eq. 16) are studied. The value of source aperture radius is assumed to be

0.025m. The same behavior is remarked as in the case of of turbulence-induced scintillation with the inner scale effect.

9.3 Beam spot radius and turbulence factor calculations

The beam spot radius at distance z from the transmitter in pure and strong turbulent atmosphere W, W_{eff} respectively are calculated by Eq. (4) and Eq. (19) for horizontal path in two cases of turbulence (strong and weak) .Fig.(8) presents comparison between W and W_{eff}. In same figure, the relation between W and W_{eff} for slant path propagation with 2000m target height is presented. Clearly, in the case of horizontal path, the difference appeared at strong turbulence more than weak turbulence. At the distance 1 km from the transmitter, the spot size of the laser beam W equals 0.031 m and W_{eff} = 0.034 m, and at the distance 10 km, W = 0.219 m and W_{eff} = 0.63 m. One can conclude that the expansion of the spot size of the beam not only depends on the distance from the transmitter, beam divergence, target and/or receiver but mainly depends on the atmospheric turbulence along the transmission range. The diffraction of the beam propagates through the strong turbulent atmosphere causes an increase in turbulence strength with increasing distance from the transmitter. In the case of a slant path, at small propagation distance and large values of target height, W and W_{eff} values converge. A pronounced effect of turbulence appears at large propagation distances. It is found that there is no much difference in the curve behavior when another target height is used. On the other hand, in the case of weak turbulence, no difference between W_{eff} and W with range in both cases, the horizontal or the slant path but the difference has shown to appear in small target height, i.e. $(h < 2000m)$

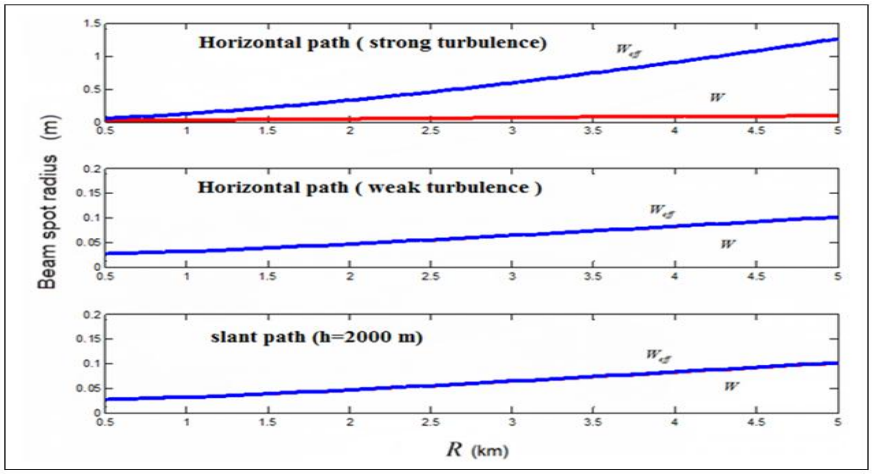

Fig. 8: Beam spot radius and effective beam spot radius vs. propagation distance.

Figures (10) (a, b) shows the feature of the turbulence factor with the range at variable receiver aperture and refractive index parameter, respectively, at zero – inner scale. The aperture transmitter radius is taken to be $W_{\circ} =$ 0.025 m. Maximum values of turbulence factor τ_{turb} are predicted at small range ($R < 0.5km$) then decreases exponentially with increasing range up to 2 km. Such decay is no longer occurs when the receiver aperture diameter is increased to $r_{rec} = 0.5m$. The significance of this competition is that the influence of turbulence is looking like the optical noise. On the other hand it is shown that the turbulence factor is inversely proportional to the beam spot radius at transmitter at a constant receiver area, and goes to minimum value at strong turbulence. This means that, high values of c_n^2, leads to minimum values of turbulence factor. These parameters should carefully be chosen for maximum received power. The same behavior is observed for the slant path propagation with no record of the effect of the target height.

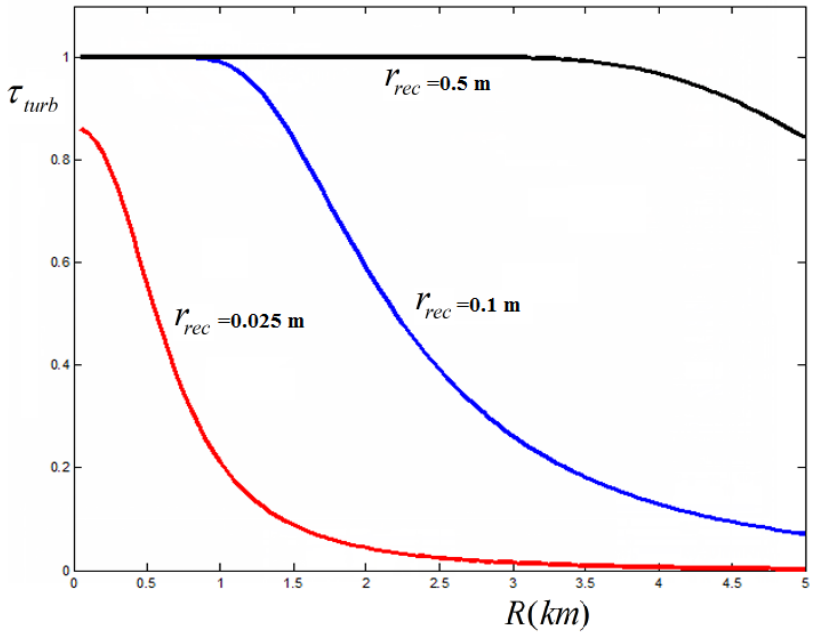

Fig.10-a: Turbulence factor in horizontal path vs. range with r_{rec} variable

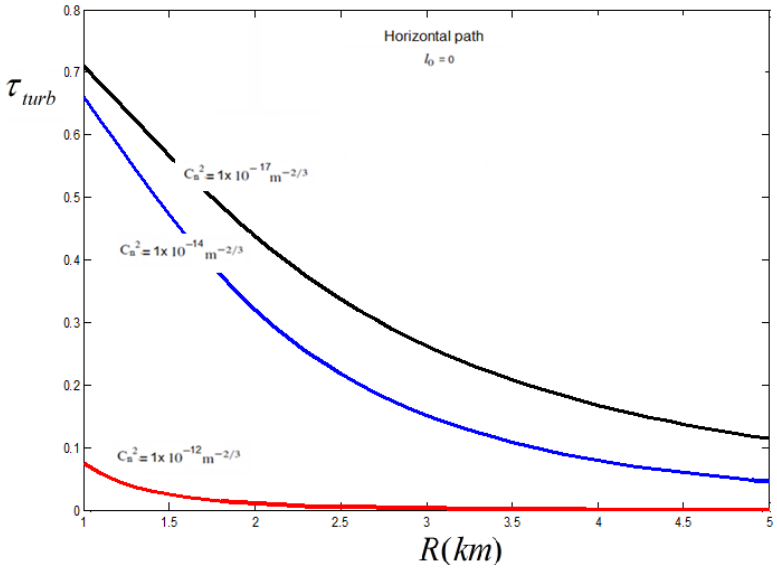

Fig.10-b: Turbulence factor in horizontal path vs. range with variable $c_n^{\,2}$

9.4 Detector received power simulation

This section focuses on the parameters which play a major role in the design simulation of the LRF and thus affecting the detector received power. The modified Eqs (33) to (35) are studied. These parameters include, the cosine angle $\cos\varphi$, beam spot radius at the transmitter $W_\circ$ and the turbulence factor τ_{turb}. It is shown that the most effective parameter on the received power is the turbulence factor, particularly at long propagation distances ($R > 2km$).

For far range calculations (Eq. 34), it is found that the calculated power is $361\mu W$ without turbulence effect reduces to $9.9\mu W$ at $R = 0.5km$ when weak turbulence is taken into consideration and reduces to $1\times10^{-4}\,\mu W$ in strong turbulence. This change increases drastically at ranges greater than $R = 0.5km$. The modified parameters are very effective in long range and less effective at short distances ($R < 0.5km$) as shown in Tables (2) and (3) which represents a comparison between received power calculated by range equations before and after modifications in two turbulence cases. The new suggested parameter is the *power*

shift ΔP_D given in tables (2) and (3). This power shifts is introduced to represent the difference in detected power, calculated by the relation [$\Delta P_D = (P_D)_{Turbulence} - (P_D)_{FreeSpace}$] in order to show the turbulence effect on the received power values at different propagation distances. Table (4) shows a comparison between the received power calculated by Gaussian beam equation in far range in absence and presence of turbulent atmosphere at different weather conditions, through slant path ($h = 0.5km$, $l_\circ = 0$) . Large decrease in the received power for the case of the ($g - g$) propagation at the same transmission distance. This appears more pronounced in Gaussian beam equation than for a far range. In addition, the maximum detectable range is significant impacted by propagation mode, and the effect of turbulence is significantly reduces the received power. According to the calculations, it makes possible to choose appropriate laser transmitted power, divergence angle, detector parameters for the optimization of the design requirements of laser rangefinder with or without turbulence. These parameters play a significant rule for the operation of laser rangefinder under different environment conditions. On the other hand , it appears that, the horizontal turbulence medium is more effective than the slant path due to the highest value of the turbulence factor in slant path than that in the case of horizontal ground propagation one.

The detector received power as a function of range in free space is shown in Fig. (11) using (g-g) propagation path with zero-inner scale ($l_\circ = 0$). A nonlinear relationship is obtained at clear weather condition ($R_v = 23km$). However, it appears that Eq. (2) is erratic, particularly, when the range is short such that the target area is larger than the light cone, the detector power becomes unrealistically large. It is shown that when R is smaller than $R_\circ = 2150m$ (bisecting point which separates between near and far range calculations), Eq. (2) produces ambiguous results, while Eq. (1) and Eq. (8) are very close, for R is larger than 2150. It is interesting to remark that the Gaussian beam range Eq. (8) reproduces the observed range much better than the conventional range Eqs. (1) and (2). In addition Eq. (8) is pivoted the need of the target area and the beam diameter required by using the conventional range equations. Another advantage of the Eq.(8) is the overridden of the discontinuity when R approaches to $R_\circ$ from left ($R \square R_\circ$) and from right ($R \square R_\circ$). It is important to note that Eq.(1) approaches to Eq.(8) at range $R_\circ$ = 2150 m , after this value, the two range equations begin to move away because of the correction factor effect of $\{1 - \exp(-2r^2{}_{tar} / \theta^2 R^2)\}$ which begins effective when the range is greater than $R_\circ$. Fig. (11) appeared identical with the experimental data given in [1, 2, and 26].

The effect of the modification factors on the received power as a function of range using the same data are shown in Figs. (12a, b). In the case of weak turbulence $c_n^{\,2} = 1 \times 10^{-17} m^{-2/3}$ and strong turbulence $c_n^{\,2} = 1 \times 10^{-12} m^{-2/3}$. As seen in the figure, the non-linear relation continued as well as abnormalities of Eq. (1) but the value of $R_\circ$ reduced from 2150 m to 2100 m in the two turbulence cases and the received power decreased in strong turbulence. As shown in figures the area before and after $R_\circ$ decreases when the correction factor is used and as a result the calculated power by using the three modified equations converges at long ranges and the received power decreases significantly due to the impact of the modification factors.

The comparison between the modified range equations (33, 34, and 35) with the new Gaussian range equation in turbulent medium (Eq.41) is made, and the typical features is shown in the Figs. (13 a, b). The comparison is done in case of strong and weak turbulence in clear weather conditions. It is shown that the received detector power estimated from new Gaussian equation is identical with that calculated for the near range at the condition of the increase in the receiver aperture and the beam spot radius at the transmitter. The advantage of new equation is in its independency of the divergence of the laser beam angle and the target radius and height in all propagation distances, and appears more refractive structure dependent which representative by W_{eff} . It is remarked that the new turbulent equation produces identical results with that reported by Kruapetch and widjaja [2], for the range ($R < 2.8km$) and for the intersection point ($R = 2.8km$) in both cases of turbulence. This confirms the validity of the model used and the approximation made for the derivation of the Gaussian range equation. Finally, Table (5) illustrates the comparison between detected power using the modified Gaussian equation and the new Gaussian. It is shown that the differences in the power values between them is very small except at distance R< 0.5km.

The power shift values, defined by $\Delta P_D = (P_{turb} - P_{free})$ are shown as expected to be negative (red shifts). The average values of ΔP_D for all turbulent cases are plotted as a function of range R (Fig.14a). It is shown the following empirical relation fits the simulation results:

$$\Delta P(\mu W) = -0.088R^6 + 1.8R^5 - 15R^4 + 62R^3 - 1.5\times10^2 R^2 + 1.8\times10^2 - 95 \quad [46]$$

Equation (46) can be considered as a metric ruler for the influence of atmospheric turbulence. Fig(14b) shows the 3D plotting between the power shifts and the turbulence factor, which are the most significant factors in describing the turbulence effect, as a function of range, and can be considered as a prototyping range explanation.

Table 2: Comparison between the received detector power in a modified form in case of **weak** turbulence

R (km)	$P_D(\mu W)$						$\Delta P_D(\mu W)\times(-1)$		
	Near range	Far range	Gaussian beam	**Modified Near range**	Modified Far range	Modified Gaussian beam	Near range	Far range	Gaussian beam
0.5	19.3	361	19.3	0.623	9.9	0.623	18.4	351	18.7
1	4.8	22	4.8	0.155	0.67	0.155	0.4	21	4.6
1.5	2.1	4	2	0.069	0.13	0.066	0.2	4.3	2.0
2	1.2	1.4	1	0.038	0.043	0.032	0.11	1.3	0.98
2.5	0.77	0.57	0.5	0.024	0.018	0.016	0.07	0.56	0.51
3	0.53	0.27	0.29	0.017	0.008	0.0094	0.052	0.27	0.29
3.5	0.39	0.15	0.17	0.012	0.0047	0.0056	0.038	0.14	0.17
4	0.30	0.08	0.02	0.0097	0.0027	0.0035	0.029	0.08	0.1
4.5	0.23	0.05	0.07	0.0076	0.0017	0.0023	0.023	0.05	0.07
5	0.19	0.03	0.05	0.0062	0.0011	0.0015	0.018	0.03	0.047

Table 3: Comparison between the received detector power in a modified form in case of **strong** turbulence

R (km)	$P_D(\mu W)$						$\Delta P_D(\mu W)\times(-1)$		
	Near range	Far range	Gaussian beam	**Modified Near range**	Modified Far range	Modified Gaussian beam	Near range	Far range	Gaussian beam
0.5	**19.3**	361	19.3	**0.006**	0.0004	0.00025	19.3	361	19.3
1	**4.8**	22	4.8	**0.0004**	0.00009	0.00006	4.8	22.6	4.8
1.5	**2.1**	4	2	**0.00008**	0.00004	0.00026	2.1	4.4	2.0
2	**1.2**	1.4	1	**0.00002**	0.00002	0.00014	1.2	1.4	1.0
2.5	**0.77**	0.57	0.5	**0.00001**	0.00001	0.000009	0.77	0.5	0.53
3	**0.53**	0.27	0.29	**0.000005**	0.000006	0.0000006	0.53	0.27	0.29
3.5	**0.39**	0.15	0.17	**0.000003**	0.000003	0.000004	0.39	0.15	0.17
4	**0.30**	0.08	0.02	**0.000002**	0.000002	0.000003	0.3	0.088	0.11
4.5	**0.23**	0.05	0.07	**0.000001**	0.000001	0.000002	0.23	0.055	0.07
5	**0.19**	0.03	0.05	**0.0000007**	0.0000009	0.0000016	0.19	0.036	0.04

Table 4: detector received power at different transmission modes

R_v (km)	R (km)	**Transmission mode**	τ_a	$P_D(\mu W)$				$\Delta P_D(\mu W)\times(-1)$	
				Gaussian beam Equation	**Far range Equation**	modified Gaussian beam Equation	**modified Far range Equation**	Gaussian beam Equation	**Far range Equation**
0.5	2	$g-g$	6.4×10^{-4}	25×10^{-7}	8×10^{-7}	1×10^{-7}	1×10^{-7}	24×10^{-7}	7×10^{-7}
		$g-a$	0.016	6×10^{-4}	4×10^{-4}	1×10^{-4}	0.52×10^{-4}	0.98×10^{-4}	3.48×10^{-4}
		$a-a$	0.17	6×10^{-2}	5×10^{-2}	1×10^{-2}	0.66×10^{-2}	5×10^{-2}	4.3×10^{-2}
	5	$g-g$	7.8×10^{-7}	4×10^{-12}	5×10^{-12}	0.09×10^{-12}	0.12×10^{-12}	7.7×10^{-12}	4.88×10^{-12}
		$g-a$	5.4×10^{-5}	18×10^{-11}	3×10^{-10}	0.4×10^{-11}	0.6×10^{-10}	5×10^{-11}	2.4×10^{-10}
		$a-a$	0.015	15×10^{-7}	2×10^{-5}	0.4×10^{-6}	0.06×10^{-5}	0.38×10^{-6}	1.9410^{-5}
10	2	$g-g$	0.81	16×10^{-1}	11×10^{-1}	2×10^{-1}	1.4×10^{-1}	1.19×10^{-1}	9.6×10^{-1}
		$g-a$	0.82	16×10^{-1}	12×10^{-1}	2×10^{-1}	1.4×10^{-1}	14.5×10^{-1}	10.6×10^{-1}
		$a-a$	0.91	2.1	15×10^{-1}	0.13	1.9×10^{-1}	1.8	13×10^{-1}
	5	$g-g$	0.59	2×10^{-2}	3×10^{-2}	0.052×10^{-2}	0.06×10^{-2}	2.3×10^{-2}	2.9×10^{-2}
		$g-a$	0.61	2×10^{-2}	3×10^{-2}	0.054×10^{-2}	0.06×10^{-2}	2.3×10^{-2}	2.8×10^{-2}
		$a-a$	0.81	4×10^{-2}	5×10^{-2}	0.054×10^{-2}	0.12×10^{-2}	4.1×10^{-2}	4.8×10^{-2}
23	2	$g-g$	0.91	2	15×10^{-1}	0.4	1.8×10^{-1}	1.7	13.2×10^{-1}
		$g-a$	0.91	2	15×10^{-1}	0.29	1.8×10^{-1}	1.8	13.2×10^{-1}
		$a-a$	0.96	2	17×10^{-1}	0.30	2.16×10^{-1}	2.02	14.8×10^{-1}
	5	$g-g$	0.80	4×10^{-2}	5×10^{-1}	0.1×10^{-2}	0.12×10^{-1}	4×10^{-2}	4.88×10^{-1}
		$g-a$	0.80	4×10^{-2}	6×10^{-2}	0.048×10^{-2}	0.12×10^{-2}	4×10^{-2}	5.8×10^{-2}
		$a-a$	0.91	5×10^{-2}	8×10^{-2}	0.061×10^{-2}	0.16×10^{-2}	5.2×10^{-2}	7.8×10^{-2}

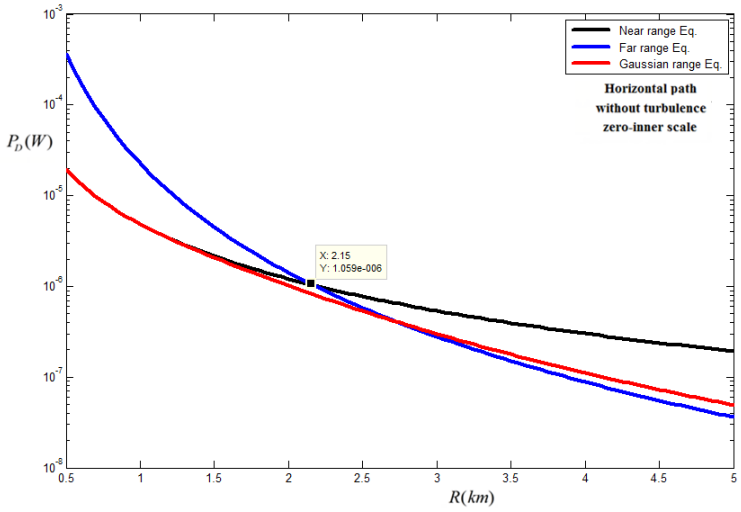

Fig.11: Detector received power vs. Range in horizontal path in free space ($l_\circ = 0$)

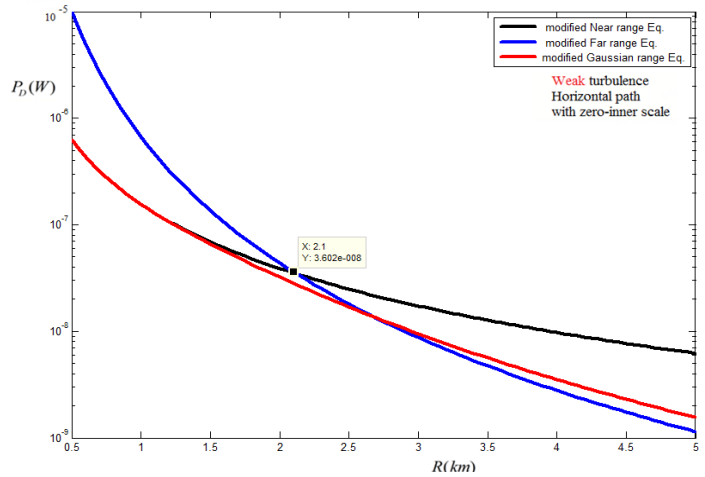

Fig. 12-a: Detector received power vs. Range in horizontal path (**weak** turbulence.)($l_{\circ} = 0$).

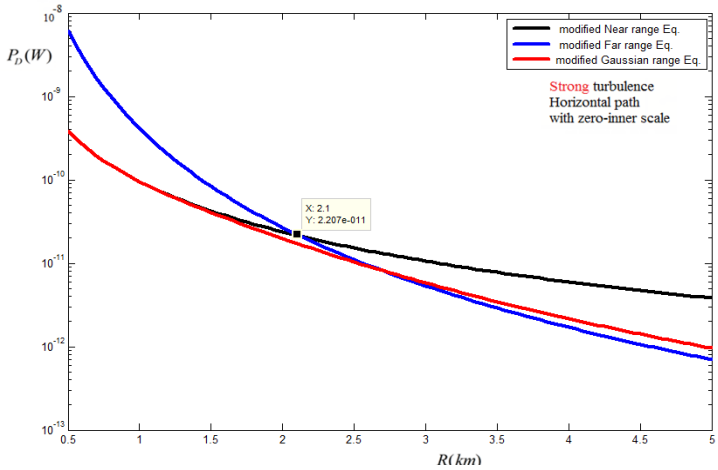

Fig. 12-b: Received power vs. Range in horizontal path (strong turbulence.)($l_{\circ} = 0$).

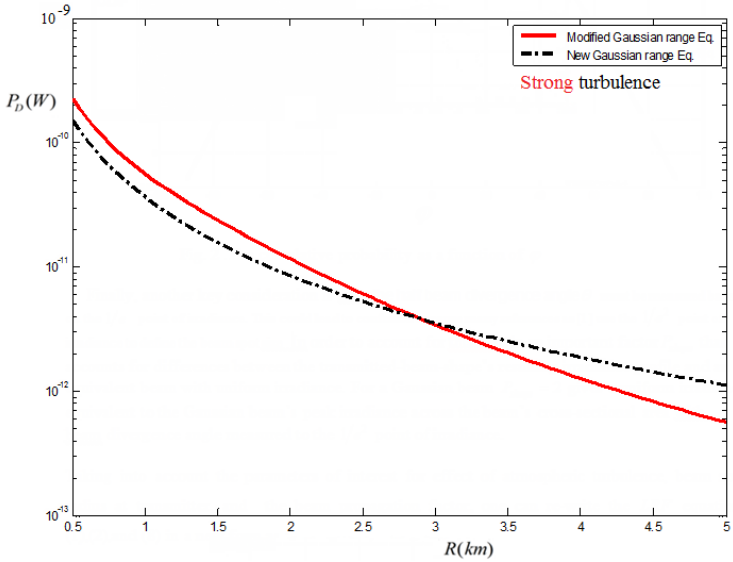

Fig (13.a) received power vs Range using the modified and the new range equations (Strong turbulence)

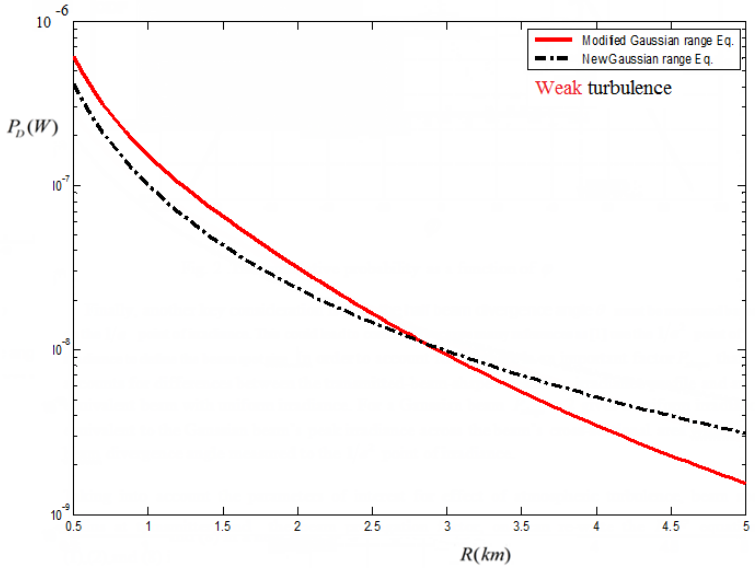

Fig.(13b): Received power vs Range using the modified and the new range equations (weak turbulence).

$$\Delta P(\mu W) = -0.088R^6 + 1.8R^5 - 15R^4 + 62R^3 - 1.5\times10^2 R^2 + 1.8\times10^2 - 95$$

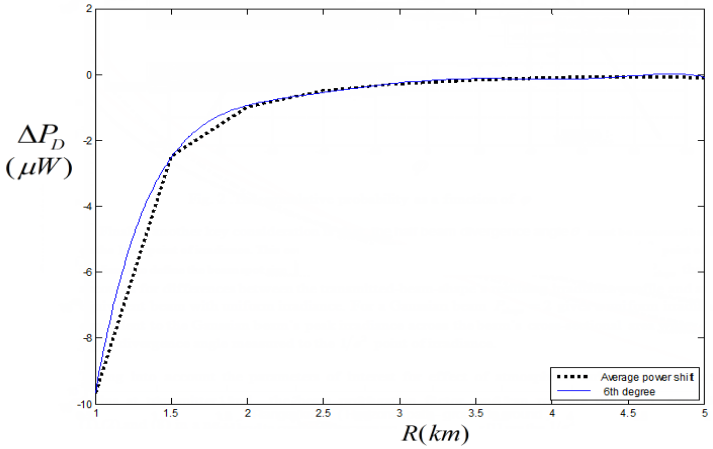

Fig. (14-a): The relation between power shift with corresponding range

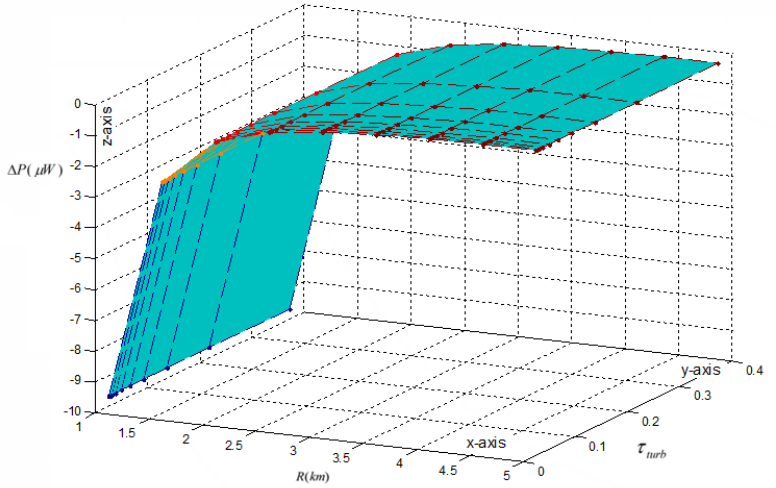

Fig. (14-b): 3D-ploting represents the relation between power shift with corresponding range and turbulence factor

10. Conclusions

The following conclusions are drawn:

a- The governing parameters for turbulence influence are c_n^2, W_0 and τ_{turb} should carefully be chosen for maximum range system design in order to reduce the turbulence influence in the optical received power.

b- The most effective parameter on the received power is the turbulence factor τ_{turb} , particularly, at long propagation distance.

c- The turbulence power shifts with respect to range can be considered as a metric ruler for the influence of turbulence.

d- The suggested new Gaussian range equation reproduces the observed data and can be considered as an alternative form to the Gaussian range equation with turbulence effects.

e- The impact of the correction factors are seen through the convergence of the range equations, particularly, for range values outside the bisecting point.

References

[1]. S. kruapech,“ Development of Eye-safe laser range finder “, Suranaree university of technology, Thesis PhD., Thailand, 2009.

[2]. S. Kruapech and J. Widjaja, "Laser range finder using Gaussian beam range equation”, Optics & Laser Technology 42 (2010) 749–754.

[3]. M. C. Amman, T. Bosch, R. Myllyla, M. Rioux,” Laser ranging: a critical review of usual techniques for distance measurement”, Optical Engineering 40(2001) 10–19.

[4]. A. A. Bazil Raj, J. A. Vijaya Selvi , and S. Durairaj , “Comparison of different models for ground-level atmospheric turbulence strength (C_n^2) prediction with a new model according to local weather data for FSO applications ”, Applied Optics , 54(2015)802-815.

[5]. W. P. Cole and M. B. Haeri, “Atmospheric-turbulence-effects correction factors for the laser range equation “, Optical Engineering, 47(2008)126001.

[6]. S. M. Augustine and N. Chetty,” Experimental verification of the turbulent effects on laser beam propagation in space “, Atmósfera 27 (2014), 385-401.

[7]. L. C. Andrews and R. L. Phillips,” Laser Beam propagation through Random Media”, SPIE, SPIE, The International Society for Optical Engineering, SPIE, 2005.

[8]. B. A. Saleh and M. C. Teich,” Beam Optics “, John Wiley & Sons, Inc., Ch.3, 1991.

[9]. A. R. Kilpela, “Pulsed time of flight laser range finder techniques for fast, high precision measurement applications “, PhD. Thesis, Oulu University, Finland, 2004.

[10]. O. Steinval, "Laser system range calculation and the Lambert W function”, Applied Optics, 48(2009) 1-7.

[11]. N. Mansharamani,” Solid-state Laserr Rngefinders A Review “, Defense Science-Journal, 45, 4(1995) 315-324.

[12]. J. Wojtanowskiw , M. Zygmunt , M. Kaszczuk , Z. Mierczk , and M.Muzal , “Comparison of 905 nm and 1550 nm semiconductor laser rangefinders’ performance deterioration due to adverse environmental conditions “ , Opto−Electronics Review 22(2009) 183–190.

[13]. W. Wen-ting, Y.Ying-ying, Z. Wei-fang, Y. Xiao-jing,” Analysis of laser atmospheric propagation characteristic and optimization of laser rangefinder”, SPIE, 8907 (2013) 890737- 890746.

[14]. L. C. Andrews, R. L. Phillips, C. Y. Hopen,” Laser Beam Scintillation with Applications”, SPIE press, USA, 2010.

[15]. J. K. Lawson and C. J. Carrano, “Using Historic Models of c_n^2 to predict and regimes affected by atmospheric turbulence for horizontal, slant and topological paths “, SPIE Optics & Photonics, San Diego, CA, USA, 2006.

[16]. D. Dirkx , R. Noomen , I. Prochazka , S. Bauer , L. Vermeersen , ” Influence of atmospheric turbulence on planetary transceiver laser ranging “,Advances in Space Research 54 (2014) 2349–2370.

[17]. A. J. Masino,” the wave structure function and the temporal frequency spread in weak and strong turbulence”, Thesis PhD., University of Central Florida, USA, 2004.

[18]. D. H. Tofsted,”Empirical modeling of laser propagation effect in intermediate turbulence “, SPIE 1487 (1991)372-381.

[19]. A. G. Alkholidi and K. S. Altowij, “Free Space Optical Communications - Theory and Practices”, CH.3, Sana'a University, Sana’a, Yemen.

[20]. J. H. Churnside, “Aperture averaging of optical scintillations in the turbulent atmosphere” Applied Optics 30 (1991), 1982-1994.

[21]. Y. Rui-Ke, C.Yuan, H. Jie, and C. Hui, "BER of Gaussian beam propagation in non-Kolmogorov turbulent atmosphere on slant path ", SPIE 8906 (2013).
[22]. P. Barbaric, M. Manojlovic," Optimization of Optical Receiver Parameters for Pulsed Laser Tracking Systems ", IEEE transactions on instrumentation and measurement 58(2009) 681-690.
[23]. L.C.Andrews, W.B.Miller,and J.C.Ricklin,"Geometrical representation of Gaussian beams propagating through complex paraxial optical system", Applied Optics 32(1993) 5918-5929.
[24]. A. Wehr, and Uwe Lohr , " Airborne laser scanning-an introduction and overview ", Journal of Photo geometry & Remote Sensing 54(1999),68-82.
[25]. S. M. Nejad and S. Olyaee," Unified Pulsed Laser Range Finder and Velocimeter using Ultra-Fast Time-To-Digital Converter", Iranian Journal of Electrical & Electronic Engineering, 5(2009)112-121.
[26]. C. Yu-dan, Z. Bing, Y. Jia-ju, M. S. juan, and Q. Xian-mei," Calculation of impulse laser rangefinders′ utmost operating range with sensitivity in different weather", Electronic & Optical Engineering Department, SPIE 9671(2015) 96710F(1-5).
[27]. A. Vain and S. Kaasalainen, "Laser Scanning, Theory and Applications ", ch.3, Estonian University of Life Sciences, Finland, 2011.
[28]. K. F. Riley, M. P. Hobson and S. J. Bence," Mathematical Methods for Physics and engineering", Cambridge University Press, 2002.
[29]. H. Li," Estimation method for maximum range of laser ranging system", Department. of Control Engineering, IEEE, 2010.
[30]. O. Bouchet, H. Sizun, C. Boisrobert, F. Favennec ," Free space Optics: Propagation and Communication " , British Library, UK, 2005.
[31]. J. Wojtanowski, M.Zygmunt, M. Traczyk, Z. Mierczyk, and M. Jakubaszek, "Beam forming optic aberrations impact on maximum range of semiconductor laser based rangefinder ", Opto-Electronics Review 22(2014) 21-30.
[32]. H. Yuksel ," Studies of the effect of atmospheric turbulence on free space optical communications" , University of Maryland, College Park, USA, Thesis PhD, 2005.
[33]. H. Buns,"System design of a pulsed laser rangefinder ",Optical Engineering,30(1991) 323-329.
[34]. R. Sabatini, M. A. Richardson, A. Gardi, and S. Ramasamy, "Airborne laser sensors and integrated systems ", Progress in Aerospace Sciences, Elsevier Ltd.(2015) .
[35]. W. Liang, Q. Chen, Y. Hho, H. Guo, and W. Zhang, "Simulation of signal-to-noise ratio for the laser range-gated imaging system ", SPIE, 9674, 967417-1, 2015.
[36]. Q. Hao, J.Cao, Y.Hu, Y.Yang, K.Li, and T.Li, "Differential optical path approach to improve signal-to-noise ratio of pulsed-laser range finding", Optical Society of America 22(2014)563-575.